Original Article

Optical imaging of stimulation-evoked cortical activity using GCaMP6f and jRGECO1a

Kicheon Park[1], Anuki C. Liyanage[1], Alan P. Koretsky[2], Yingtian Pan[1], Congwu Du[1]

[1]Department of Biomedical Engineering, Stony Brook University, Stony Brook, NY, USA; [2]Laboratory of Functional and Molecular Imaging, National Institute of Neurological Disorders and Stroke, National Institutes of Health, Bethesda, MD, USA

Correspondence to: Congwu Du, PhD. Professor, Department of Biomedical Engineering, State University of New York at Stony Brook, Life Science Bldg, Rm. 002, Stony Brook, NY 11794-5281, USA. Email: Congwu.Du@stonybrook.edu.

Background: Genetically encoded calcium indicators (GECIs), especially the GCaMP-based green fluorescence GECIs have been widely used for *in vivo* detection of neuronal activity in rodents by measuring intracellular neuronal Ca^{2+} changes. More recently, jRGECO1a, a red shifted GECI, has been reported to detect neuronal Ca^{2+} activation. This opens the possibility of using dual-color GECIs for simultaneous interrogation of different cell populations. However, there has been no report to compare the functional difference between these two GECIs for *in vivo* imaging. Here, a comparative study is reported on neuronal responses to sensory stimulation using GCaMP6f and jRGECO1a that were virally delivered into the neurons in the somatosensory cortex of two different groups of animals, respectively.

Methods: GCaMP6f and jRGECO1a GECI were virally delivered to sensory cortex. After 3–4 weeks, the animals were imaged to capture the spatiotemporal changes of neuronal Ca^{2+} and the hemodynamic responses to forepaw electrical stimulation (0.3 mA, 0.3 ms/pulse, 0.03 Hz). The stimulation-evoked neuronal Ca^{2+} transients expressed with GCaMP6f or jRGECO1a were recorded during the baseline period and after an acute cocaine administration (1 mg/kg, i.v.).

Results: Histology confirmed that the efficiency of jRGECO1a and GCaMP6f expression into the cortical neurons was similar, i.e., 34%±3% and 32.7%±1.6%, respectively. Our imaging *in vivo* showed that the hemodynamic responses to the stimulation were the same between jRGECO1a and GCaMP6f expressed groups. Although the stimulation-evoked fluorescence change (ΔF/F) and the time-to-peak of the neuronal Ca^{2+} transients were not significantly different between these two indicators, the full-width-half-maximum (FWHM) duration of the ΔF/F rise in the jRGECO1a-expressed group (0.16±0.02 s) was ~50 ms or 46% longer than that of the GCaMP6f group (0.11±0.003 s), indicating a longer recovery time in jRGECO1a than in GCaMP6f transients ($P<0.01$). This is likely due to the longer off rate of jRGECO1a than that of GCaMP6f. After cocaine, the time-to-peak of Ca^{2+} transients was delayed and their FWHM duration was prolonged for both expression groups, indicating that these are cocaine's effects on neuronal Ca^{2+} signaling and not artifacts due to the property differences of the GCEIs.

Conclusions: This study shows that both jRGECO1a and GCaMP6f have sufficient sensitivity for tracking single-stimulation-evoked Ca^{2+} transients to detect neuronal activities from the brain. Since these GECIs are emitted at the different wavelengths, it will be possible to use them together to characterize the activity of different cell types (e.g., neurons and astrocytes) to study brain activation and brain functional changes in normal or diseased brains.

Keywords: Cocaine; GCaMP fluorescence imaging; jRGECO1a fluorescence imaging; Ca^{2+} transient

Submitted Jul 29, 2020. Accepted for publication Sep 24, 2020.
doi: 10.21037/qims-20-921
View this article at: http://dx.doi.org/10.21037/qims-20-921

Introduction

Fluorescence Ca^{2+} indicators have played an important role in understanding cellular signaling, especially in the brain. These indicators have made it possible to optically detect cellular Ca^{2+} concentration changes and to track cellular activity across multiple spatial scales from a single synapse to a neuronal population (1-3). In general, there are two types of Ca^{2+} indicators: chemical Ca^{2+} indicators and protein based genetically encoded Ca^{2+} indicators (GECIs) (4). For brain functional studies, the GECIs are now preferred because specific delivery to targeted cell types can be controlled (1,3). For example, GCaMP6, a green fluorescence GECI, has been widely used for measuring neuronal activity (1,5-7) because of its high sensitivity to detect neuronal Ca^{2+} transients, and under some conditions even to detect a single Ca^{2+} transient arising from a single action potential (8). However, the excitation and emission of the GCaMP GECIs are all within blue and green wavelength range, where both scattering and absorption of biological tissue are relatively high (8,9). The property differences among the GECIs such as different kinetics (e.g., different Ca^{2+} on-and-off rates) always raise the question of whether the Ca^{2+} changes are to some extent influenced by their properties; therefore, it is necessary to compare the results using different GECIs. Furthermore, many GFP-based transgenic rodent models (8) share the same green fluorescence emission with the green GECIs (e.g., GCaMP serials), which makes difficult to use such green GECIs for Ca^{2+} imaging for these animals. There are many occasions where it would be important to concurrently track the activities of different cell types from the same animal, for example to image the Ca^{2+} activities from neurons and astrocytes in response to a brain stimulation.

Different color GECIs, such as jRGECO1a, red GECI, have been developed to increase the utility of GECIs (8). While the chemical property and the fluorescent characteristics of jRGECO1a have been described (8), there is no report on side-by-side comparison between red and green GECIs for Ca^{2+} transients *in vivo*. The goal of this study was to compare the performance of a green GECI (GCaMP6f) with a red GECI (jRGECO1a) for brain functional imaging. Specifically, jRGECO1a and GCaMP6f were virally delivered into the somatosensory cortex to express the neurons in two different groups of rats, respectively. After 3–4 weeks, optical imaging was conducted over the cortex of each animal during which the synchronized neuronal Ca^{2+} transients and the hemodynamic responses to a sensory stimulation (i.e., electrical stimulation of the forepaw) were acquired. The results between the jRGECO1a and GCaMP6f animal groups were analyzed to characterize their differences.

Cocaine produces neural deficits (10) when abused repetitively in humans. For example, Lee *et al.* 2003 (11) showed that the maximal response of brain to visual stimulation frequency shifted from 4 to 8 Hz between controls and cocaine abusers, suggesting that due to cocaine-induced deficits more intense 'stimuli' were needed for a cocaine abuser to 'trigger' the brain to function 'normal'. It has been reported recently that cocaine abusers have widespread disruption in brain fMRI activation patterns in response to a working memory task (12). In addition, animals with extended access to cocaine show cortical deficits along with the compulsivity (13). Here, we applied these two GECIs to study the cocaine's effects on neuronal activities from the cortex *in vivo*. The Ca^{2+} fluorescence transient (neuronal response) to the forepaw stimulation mimics a sensory stimulus in humans. Studying the high temporal resolution of these Ca^{2+} signals will help us to understand the mechanisms that underlie the abnormal brain function due to the neuronal deficits induced by cocaine.

Methods

Animals

Male Sprague Dawley (SD) rats (n=7) were used in the study. The genetically-encoded Ca^{2+} indicators, AAV.Syn.GCaMP6f.WPRE.SV40 (n=4) and AAV.Syn.NES-jRGECO1a.WPRE.SV40 (n=3) were virally delivered into the somatosensory cortex (A/P: +0.5, M/L: +3.0, Depth: 1.2) of rats in Dr Koretsky's laboratory at NIH. Three weeks after viral injection, the rats were shipped to Stony Brook University for *in vivo* imaging studies. All experiment procedures were approved by the Institutional Animal Care and Use Committees (IACUC) of NIH and Stony Brook University and were performed in accordance with the National Institutes of Health Guide for the Care and Use of Laboratory Animals.

Experimental preparation and surgical procedure

After 3–4 weeks of viral incubation, animals were used for optical imaging studies. Before imaging, the animal was intubated and mechanically ventilated (CWE, SAR-830/

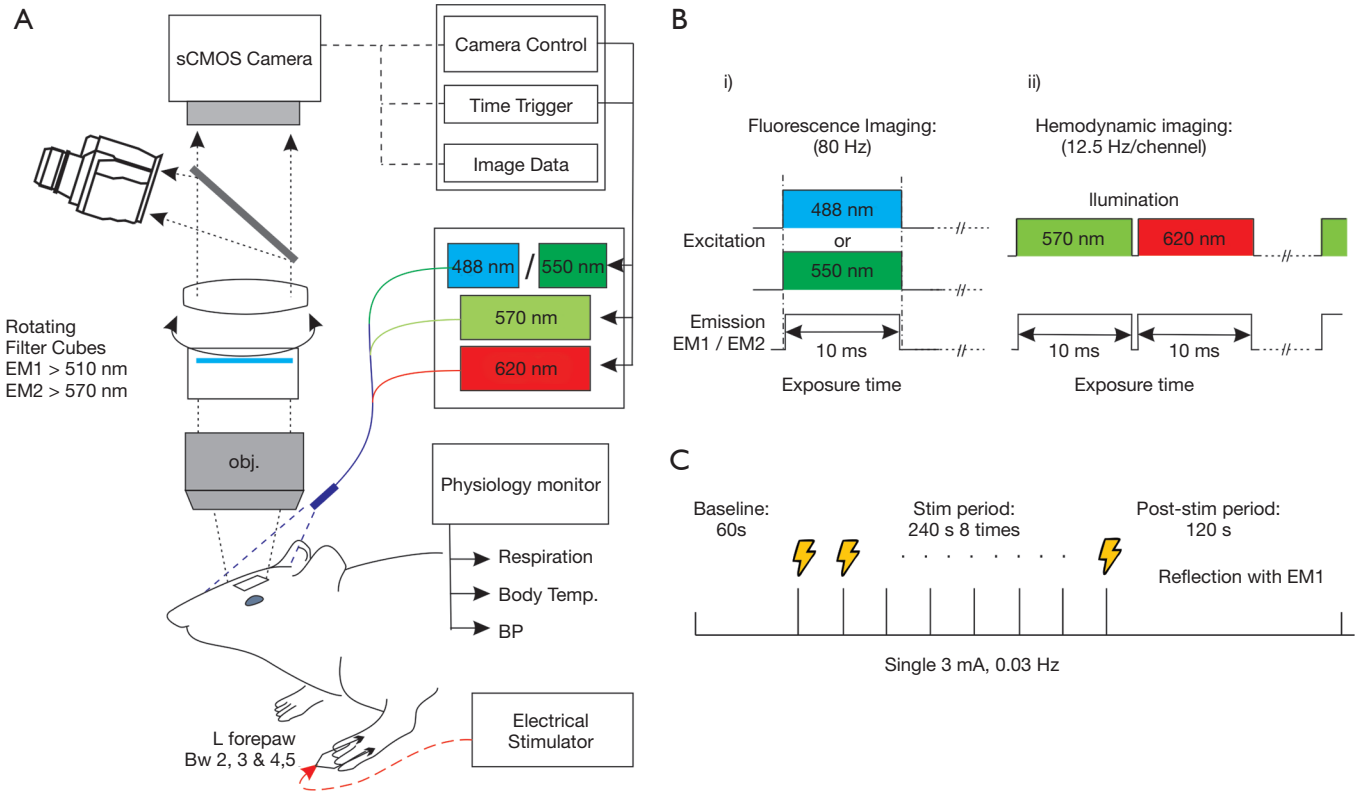

Figure 1 A Sketch to illustrate the optical imaging setup and the experimental protocol. (A) Multimodality imaging platform (MIP) to image the neuronal Ca^{2+} fluorescence and hemodynamic changes in response to forepaw electrical stimulation. (B) Fluorescence imaging approach for GCaMP6f or jRGECO1a detection (i) and reflection imaging to detect Hemodynamic changes (ii). (C) Paradigm for on the forepaw stimulation during the experiment.

P) and anesthesia was maintained with 2–3% isoflurane in a mix of 70% oxygen: 30% air. The physiology of the animal, including body temperature, respiration, blood pressure, and partial pressure of carbon dioxide (pCO_2) were continuously monitored to ensure normoxia. The left femoral artery was cannulated for blood pressure monitoring (Small Animal instrument Inc. SA monitoring System, Model 1025) and periodical blood gas sampling (Radiometer America, ABL80 FLEX), whereas the left femoral vein was catheterized for drug administration (e.g., α-chloralose anesthetic). The rat was then positioned in a stereotaxic frame (Kopf 900, Tujunga, CA, USA) and a cranial window (~4×5 mm^2, *Figure 1A*) was created on the right somatosensory cortex (A/P: +0.5 mm, M/L: +3.0 mm). The dura was carefully removed, and a thin glass coverslip was cemented after 1.25% agarose gel was applied on cortical surface. After the surgery, the animal was transferred to the imaging platform and two electrodes were inserted under the skin of the left forepaw in the space between digits 2 to 3 and between digits 4 to 5 (*Figure 1A*). Anesthesia was switched from isoflurane to α-chloralose for functional brain imaging using an initial bolus of 50 mg/kg, followed by a continuous infusion of 25 mg/kg/hr through the femoral vein. The paradigms of light source and imaging acquisition are illustrated in *Figure 1B*, the illumination and detection were synchronized by using home-developed LabVIEW program. For sensory stimulation, electrical stimuli (A-M System 2100, Sequim, WA, USA) were delivered through a pair of electrodes implanted under the skin of the forepaws with a 0.03 Hz/3 mA single-stimulus (*Figure 1C*). Stimuli were synchronized with image acquisition using a custom LabVIEW program.

In vivo time-lapse optical imaging

A custom multimodality optical imaging platform (*Figure 1A*) was used for imaging neuronal Ca^{2+} fluorescence (λ_{Ex}=488 nm for GCaMP6f, λ_{Ex}=550 nm for jRGECO1a), and the blood volume/total hemoglobin (HbT) (14) from

rat cortex over a large field of view (~4×5 mm^2). A multi-channel light engine (Spectra Light Engine, Lumencor), synchronized with a sCMOS camera (Zyla4.2, Andor, pixel size =6.5 μm), was coupled into a fiber bundle to sequentially deliver multispectral light to illuminate rat brain through the cranial window. For imaging of forepaw stimulation, fluorescent Ca^{2+} transients were captured at 80 frames per second [fps, *Figure 1B* (i)] and multichannel images of λ_1=570 nm and λ_2=620 nm were captured at 12.5 fps [*Figure 1B* (ii)] to detect the hemodynamic changes evoked by the sensory stimulation (15,16). The emission filter set EM1 (≥510 nm) was used for GCaMP6f Ca^{2+} fluorescence imaging and hemodynamic detection via time-sharing LED illuminations, whereas the emission filter EM2 (≥570 nm) was used for jRGECO1a Ca^{2+} fluorescence imaging.

The regions of interests (ROIs) for Ca^{2+} fluorescence and hemodynamic responses were selected within the activated brain regions in the somatosensory cortex. The hemodynamic changes, ΔHbT in response to the stimulation were determined based on the multichannel images reflected at λ_1=570 nm and λ_2=620 nm. The detailed quantification, which was described previously (15,16), can be given as

$$\begin{bmatrix}\Delta HbO_2\\ \Delta HbR\end{bmatrix}=\begin{bmatrix}\varepsilon_{HbO_2}^{\lambda_1}\varepsilon_{HbR}^{\lambda_1}\\ \varepsilon_{HbO_2}^{\lambda_2}\varepsilon_{HbR}^{\lambda_2}\end{bmatrix}^{-1}\times\begin{bmatrix}\ln\left(\frac{R_{\lambda_1}(0)}{R_{\lambda_1}(t)}\right)/L_{\lambda_1}(t)\\ \ln\left(\frac{R_{\lambda_2}(0)}{R_{\lambda_2}(t)}\right)/L_{\lambda_2}(t)\end{bmatrix} \quad [1]$$

where $\varepsilon_{HbO_2}^{\lambda_1}$, $\varepsilon_{HbR}^{\lambda_2}$, $\varepsilon_{HbO_2}^{\lambda_2}$, $\varepsilon_{HbR}^{\lambda_1}$ are the molar extinction coefficients for oxygenated-(HbO_2) and deoxygenated-(HbR) hemoglobin; R_{λ_1}, R_{λ_2} are diffuse reflectances at the wavelengths of 570 and 620 nm, respectively; L_{λ_1}, L_{λ_2} are path lengths of light propagation (17). Then, ΔHbT can be determined as the sum of ΔHbO_2 and ΔHbR,

$$\Delta HbT = \Delta HbO_2 + \Delta HbR \quad [2]$$

The relative changes in Ca^{2+} fluorescence change (ΔF/F) were obtained after correcting the local HbT changes due to the light absorbance changes within the tissue via ratiometric analysis (16,18,19).

Cocaine administration

To assess the cocaine's effects on neuronal Ca^{2+} signaling, the animal received an acute cocaine challenge (1 mg/kg, i.v.) after the baseline stimulation experiments. At ~8 min post cocaine administration, forepaw stimulations were repeated and the stimulation evoked Ca^{2+} transients in the cortex were recorded and compared with those obtained during the baseline period.

Ex vivo imaging to evaluate the efficiency of viral expression

After *in vivo* imaging, the animals were perfused with 0.1 M PBS (pH 7.4) followed by fixation in 4% paraformaldehyde. Through immunostaining, neurons were identified using a mouse anti-NeuN primary antibody. The total neurons were visualized with a goat anti-mouse Alexa Fluor 488 or Alexa fluor 594 secondary evaluation of GCaMP6f and jRGECO1a expressions, respectively. The ratio of jRGECO1a- and GCaMP6f- expressing neurons over the total neurons (e.g., NeuN positive cells) within the cortex were assessed by confocal fluorescence microscopy.

Quantification and statistics

All data are presented as means ± SEM. To compare the fluorescence Ca^{2+} transients between jRGECO1a- and GCaMP6f-expressing neurons, the following two parameters of the Ca^{2+} signals were assessed: the full-width-half-maximum (FWHM) duration and the time to peak (from stimulation onset to time point of the maximum) of the Ca^{2+} transient responses. For quantifying hemodynamic response (ΔHbT), the parameters of latency (delay of response form stimulation onset) and the FWHM duration of the ΔHbT changes evoked by stimulation were computed. Comparison of two different groups (e.g., GCaMP6f- and jRGECO1a-expressing animal groups) was analyzed using Student's *t*-test. In all tests, $P<0.05$ was considered statistically significant.

Results

Expression of GCaMP6f and jRGECO1a into Neurons

To compare the fluorescence Ca^{2+} transients of neurons expressed with GCaMP6f or jRGECO1a, a viral injection approach was used to deliver them into the somatosensory cortex of two groups of animals as shown in *Figure 2A*. A 0.4 μL of AAV.Syn.GCaMP6f.WPRE.SV40 or AAV.Syn.NES-jRGECO1a.WPRE.SV40 was injected into forepaw somatosensory cortex of group 1 or group 2 of animals. *Figure 2B* shows *in vivo* fluorescence images obtained from the cortices of GCaMP6f- and jRGECO1a-expressed

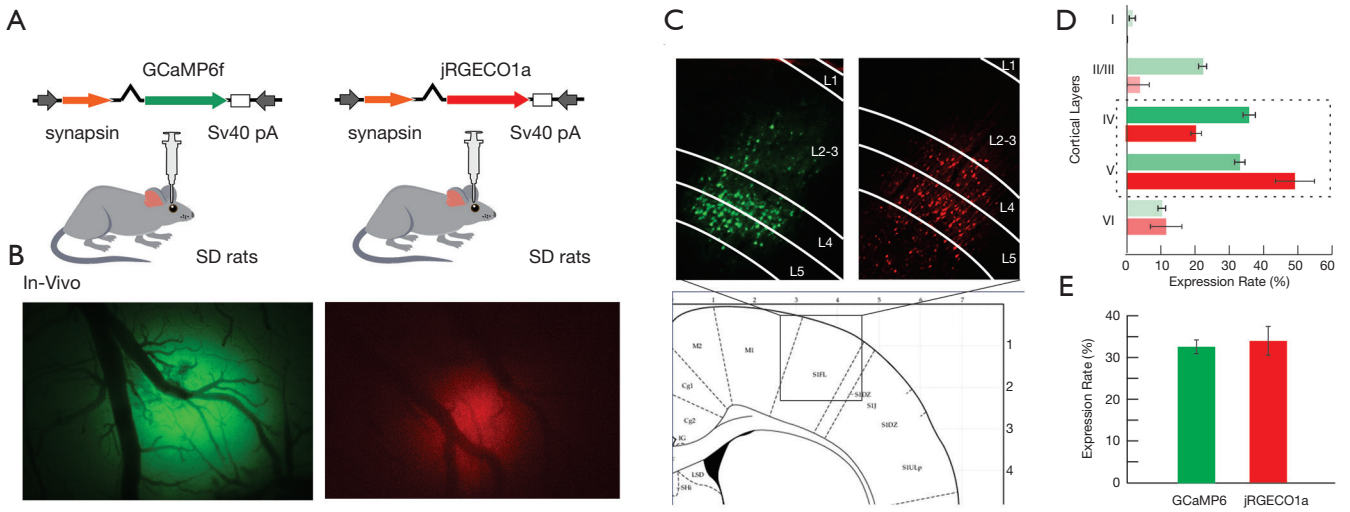

Figure 2 GCaMP6f-, jRGECO1a- expression in neurons within the somatosensory cortex. (A) Viral injection procedure to express jRGECO1a or GCaMP6f in neurons within somatosensory cortex; (B) *in vivo* image of neuronal Ca^{2+} fluorescence from rat cortex with GCaMP6f and jRGECO1a, respectively; (C) *ex vivo* confocal fluorescence images, showing the neurons expressing GCaMP6f or jRGECO1a in the cortex; (D) distribution of jRGECO1a- or GCaMP6f-expressing neurons in different cortical layers as the ratio between fluorescence expressed neuron counts versus the total neuron counts in each cortical layer; (E) comparison of percentage of jRGECO1a- or GCaMP6f-expressing rates in the cortex, showing no significant difference in their expression efficiency.

animals, respectively. *Figure 2C* shows fluorescence images of the brain sections from these two animal groups confirming the viral expressions in the somatosensory cortex. *Figure 2D* shows the distributions GCaMP6f- or jRGECO1a-expressing neurons as a function of cortical depth of the brains obtained from the GCaMP6f and jRGECO1a animals, which indicates the neuronal uptakes of Ca^{2+} indicators were mostly in the layers IV-V. *Figure 2E* compares the quantification of neuronal uptakes of GCaMP6f (32.7%±1.6%, n=4) and jRGECO1a (34%±3%, n=3). This result shows no significant difference in the expression efficiency into the neurons in the somatosensory cortex between GCaMP6f and jRGECO1a animals (P=0.65).

Spatiotemporal Ca^{2+} transients and hemodynamic responses to forepaw stimulation

Figure 3 represents stimulation-evoked spatiotemporal Ca^{2+} transients of GCaMP6f-expressing neurons and the hemodynamic (i.e., HbT) changes in the somatosensory cortex evoked by forepaw electrical stimulation pulse train (3 mA/0.03 Hz/0.3 ms). As illustrated in *Figure 3A,B*, the sensory stimulation was repeated nine times during the imaging period, and the stimulation-evoked Ca^{2+} transients and ΔHbT responses were synchronized with the stimulation pulses, thus indicating that our imaging setup has sufficient sensitivity to detect single stimulation-evoked neuronal and hemodynamic activations from the brain *in vivo*. *Figure 3C* shows the time-lapse images of a Ca^{2+} fluorescence transient evoked by the stimulation at t=0s. *Figure 3D* plots the Ca^{2+} transients to single stimuli (dashed green traces) synchronized to the stimuli onsets at t=0 s (vertical line) and their average trace (bold green trace), which shows that the ΔF/F increased after the stimulation and the time to peak was at 35±2.1 ms. The peak fluorescence increase was ΔF/F=12.34%±1.1% and the FWHM duration of the Ca^{2+} transient was 101±6.8 ms (gray shadow area) for GCaMP6f-expressing neurons. The hemodynamic response to the stimulation (i.e., ΔHbT) is illustrated in *Figure 3E*, in which the latency to stimulation was 1.61±0.11 s, the time to peak was 5.58±0.17 s, and the FWHM duration was 4.44±0.25 s. These results were consistent with the facts that the hemodynamic response is much slower than the Ca^{2+} response due to the complexities of neurovascular coupling and that the surface venous vascular compartment dominates the HbT measurement (19-24).

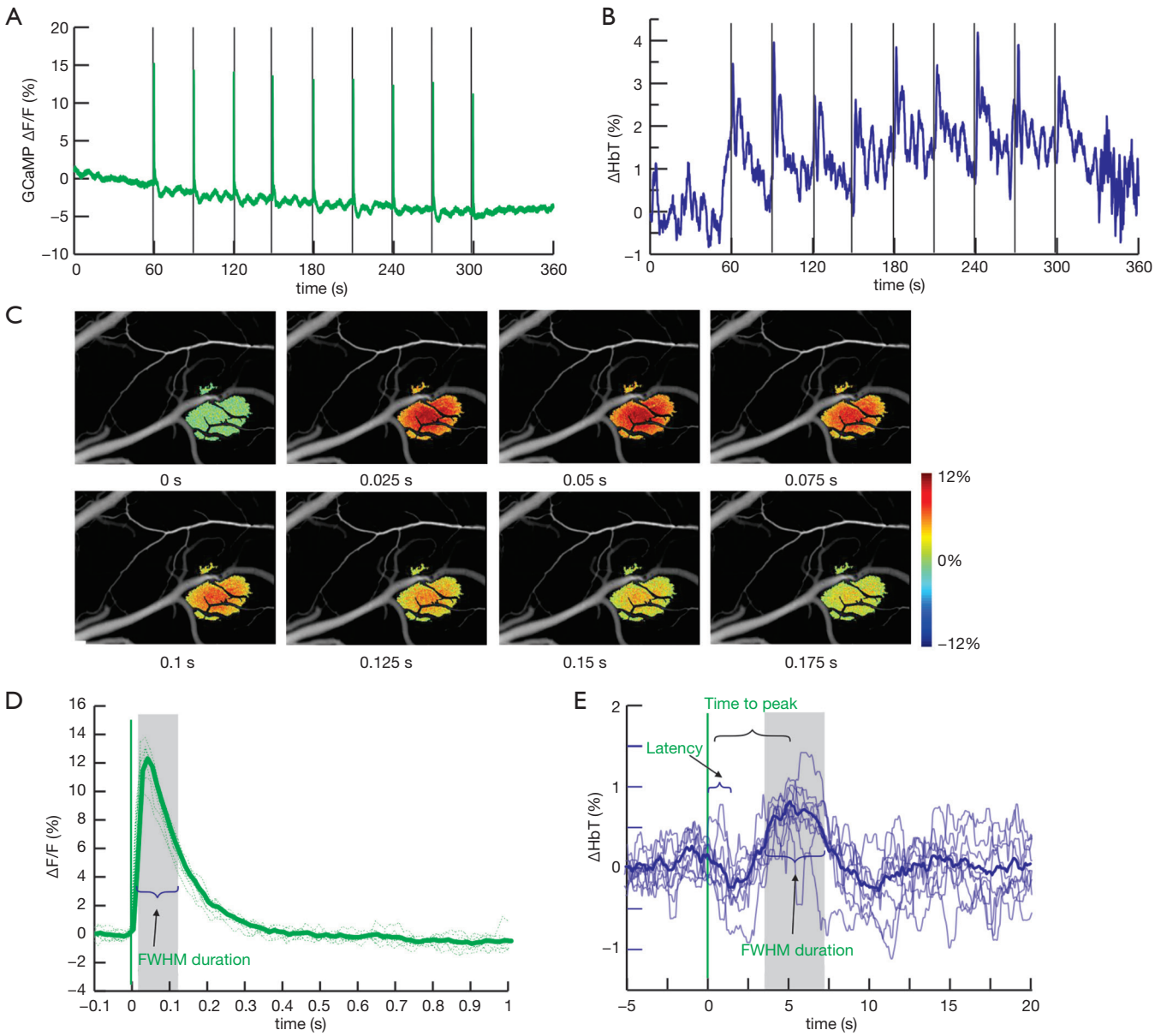

Figure 3 Ca^{2+} transients of GCaMP6f-expressing neurons and the hemodynamic responses to sensory electrical stimulation. (A) Fluorescence Ca^{2+} transients (ΔF/F) evoked by a forepaw electrical stimulation train (3 mA/0.3 ms/0.03 Hz); (B) the corresponding hemodynamic changes (ΔHbT); (C) time-lapse images of Ca^{2+} fluorescence changes evoked by a sensory stimulation; (D) temporal profile of transient Ca^{2+} response to single forepaw stimuli in which the dashed traces were individual transients (n=1, m=7) synchronized with the stimuli at t=0 s and the solid trace was their average; (E) temporal profile of the ΔHbT response (dashed traces, n=4, m=16) and their average (solid trace), in which the latency, time to peak and FWHM duration of ΔHbT are illustrated. Black-lines in A and B illustrate stimulation pulses.

Figure 4 represents stimulation-evoked spatiotemporal Ca^{2+} transients of jREGCO1a-expressing neurons and the hemodynamic responses to sensory stimulation pulse train. *Figure 4A,B* shows the stimulation-evoked Ca^{2+} transients and ΔHbT responses synchronized with the stimulation pulses. *Figure 4C* shows the time-lapse images of a Ca^{2+} fluorescence transient evoked by the stimulation at t=0 s. *Figure 4D* plots the Ca^{2+} transients to single stimuli (dashed red traces) superimposed on the stimuli onsets at t=0 s (vertical line) and their average trace (bold red trace), which

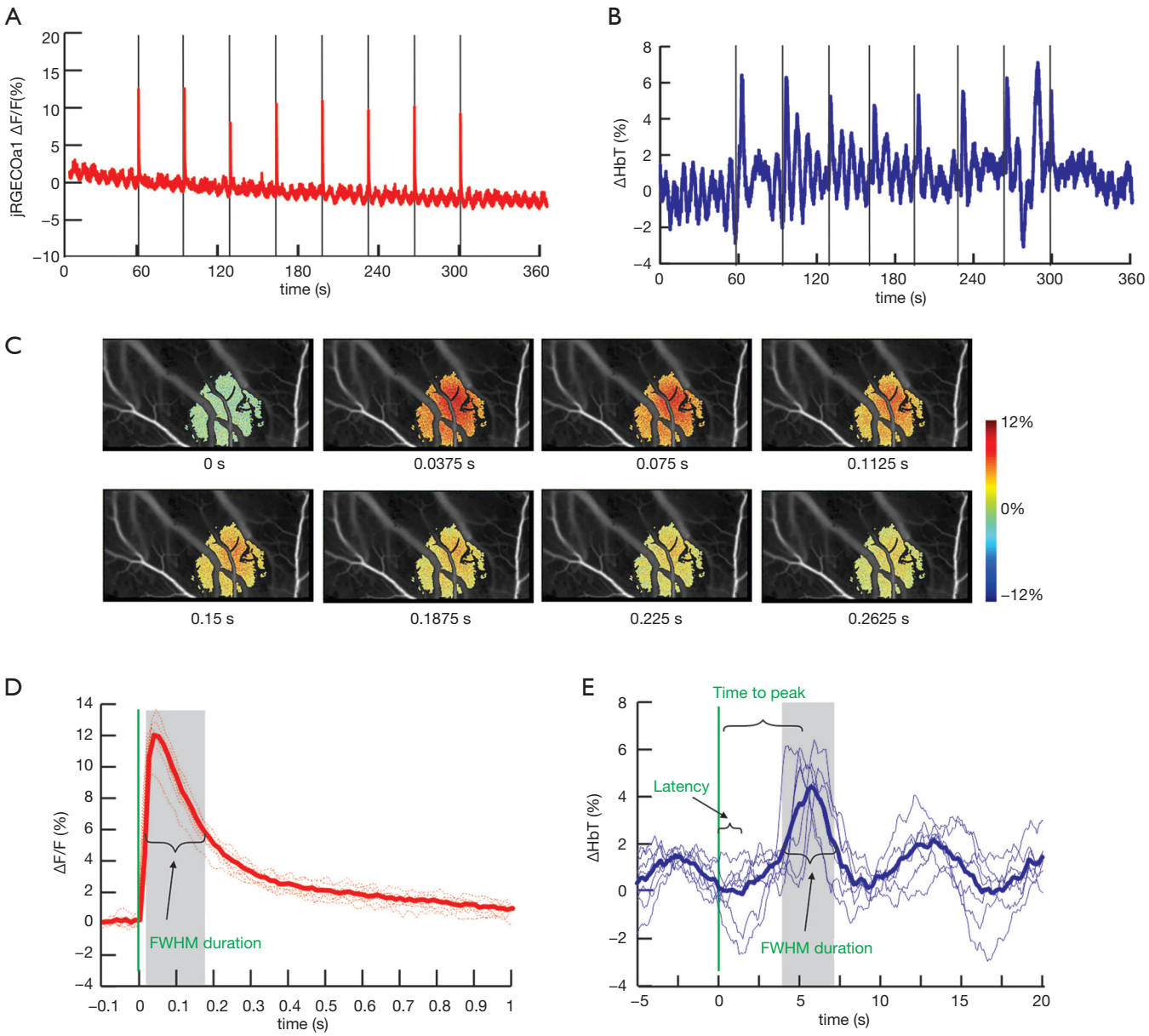

Figure 4 Ca^{2+} transients of jRGECO1a-expressing neurons and the hemodynamic responses to sensory electrical stimulation. (A) Fluorescence Ca^{2+} transients (ΔF/F) evoked by a forepaw electrical stimulation train (3 mA/0.3 ms/0.03 Hz); (B) the corresponding hemodynamic changes (ΔHbT); (C) time-lapse images of Ca^{2+} fluorescence changes evoked by a sensory stimulation; (D) temporal profile of transient Ca^{2+} response to single forepaw stimuli in which the dashed traces were individual transients (n=1, m=8) synchronized with the stimuli at t=0 s and the solid trace was their average; (E) temporal profile of the ΔHbT response (dashed traces, n=3, m=14) and their average (solid trace), in which the latency, time to peak and FWHM duration of ΔHbT are illustrated. Black-lines in A and B illustrate stimulation pulses.

shows that the ΔF/F increased after the stimulation and the time to peak was at 42±2.2 ms. The peak fluorescence change was ΔF/F=12.25%±0.38% and the FWHM duration of the Ca^{2+} transient was 148±4.4 ms (gray shadow area) for the jREGCO1a-expressing neurons. *Figure 4E* shows the ΔHbT responses evoked by the single stimuli, in which the latency to stimulation was 1.88±0.14s, the time to peak was 5.22±0.17 s, and the FWHM duration was 4.44±0.25 s.

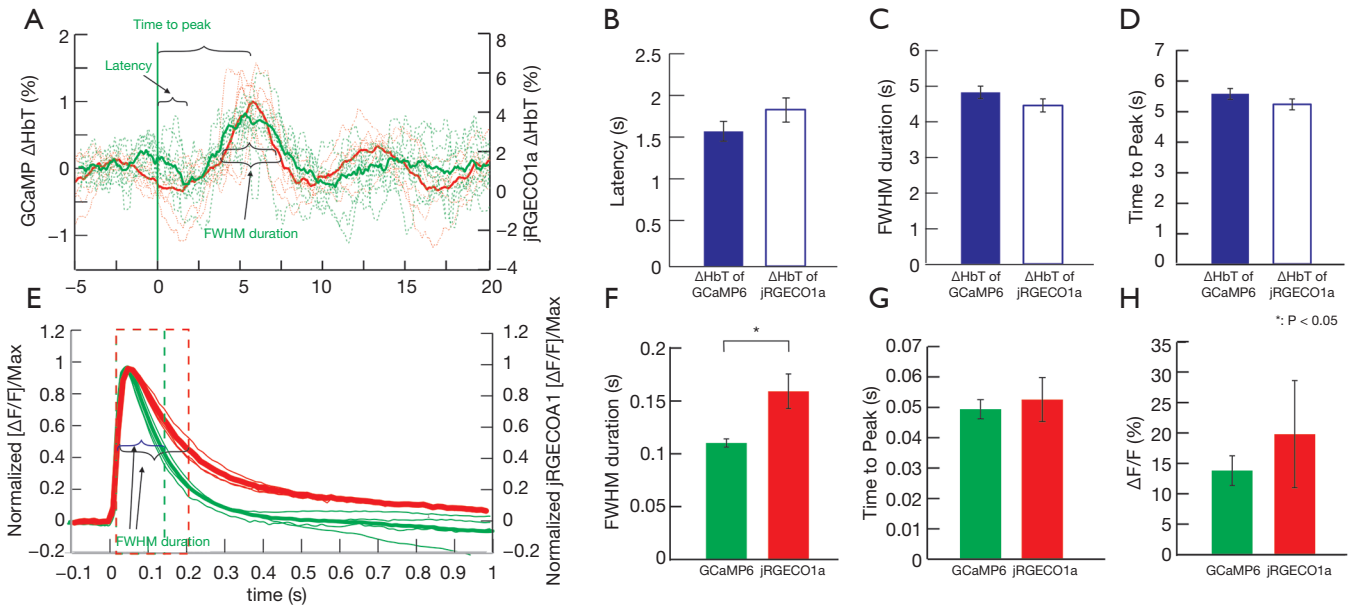

Figure 5 Comparison of single sensory stimulation evoked Ca^{2+} transients in GCaMP6f-expressed rats (n=4) and jRGECO1a-expressed rats (n=3) and the hemodynamic responses. (A) Superposed ΔHbT responses to the stimuli between GCaMP6f- and jRGECO1a-expressed animals; (B,C,D) latency, full-width-half-maximum duration, and time to peak of ΔHbT in GCaMP6f- (blue) and jREGCO1a- (white) rats; (E) superposed Ca^{2+} fluorescence transients (ΔF/F) in response to the stimuli between GCaMP6f- and jRGECO1a-expressed animals; (F,G,H) FWHM duration, time to peak, and peak ΔF/F of fluorescence Ca^{2+} transients in GCaMP6f- (green) and jREGCO1a- (red) rats.

A comparison with the results in *Figure 3* indicates that both red GCaMP6f and red jRGECO1a GECIs enables detection and quantification of neuronal activities evoked by a single sensory stimulation.

Figure 5 summaries the comparison of the sensory stimulation evoked Ca^{2+} transients (ΔF/F) and the hemodynamic responses (ΔHbT) between the GCaMP6f-expressed rats (n=4) and the jRGECO1a-expressed rats (n=3). The superposed ΔHbT changes and Ca^{2+} fluorescence transients (ΔF/F) in response to the stimuli were illustrated in *Figure 5A* and *E*, respectively. As expected, no significant differences were found in the ΔHbT responses between the two group as shown in *Figure 5B,C,D*. The latency between GCaMP6f and jRGECO1a animals was 1.62±0.12 *vs.* 1.88±0.14 s (P=0.16), the FWHM duration was 4.81±0.17 *vs.* 4.44±0.25 s (P=0.29), and the time to peak was 5.58±0.2 *vs.* 5.22±0.2 s (P=0.23). For neuronal Ca^{2+} transients, however, the FWHM duration (*Figure 5F*) in the jRGECO1a animals was 0.16±0.02 s, which was significantly longer than that of 0.11±0.003 s in the GCaMP6f animals (P<0.01). The time to peak in jRGECO1a and GCaMP6f animals (*Figure 5G*) was 0.05±0.007 *vs.* 0.049±0.003 s (P=0.6), the peak Ca^{2+} transient amplitude was 13.8%±2.4% *vs.* 19.8%±8.8% (P=0.48), both of which were not significantly different.

Cocaine induced neuronal Ca^{2+} dynamic responses in GCaMP6f vs. jREGCO1a animals

Figure 6 summarizes the effects of acute cocaine administration (1 mg/kg, i.v.) on stimulation-evoked neuronal Ca^{2+} transients in GCaMP6f- *vs.* jRGECO1a-expressing rats, respectively. Specifically, *Figure 6A,B* show the temporal profiles of sensory stimulation evoked Ca^{2+} transients at baseline (solid traces) and after cocaine (dashed traces), which were delayed and prolonged by cocaine in both groups. Statistical analyses on the cocaine's effects are summarized in *Figure 6C,D*. The results indicate that the FWHM duration and the time-to-peak of Ca^{2+} transients were significantly increased from 0.11±0.003 to 0.13±0.003 s (P=0.01, n=4) and from 0.05±0.007 to 0.09±0.008 s (P=0.04, n=4) for the GCaMP6f rats. Similarly, the FWHM duration and the time-to-peak of Ca^{2+} transients were significantly increased from 0.159±0.01 to 0.26±0.03 s (P=0.03, n=3)

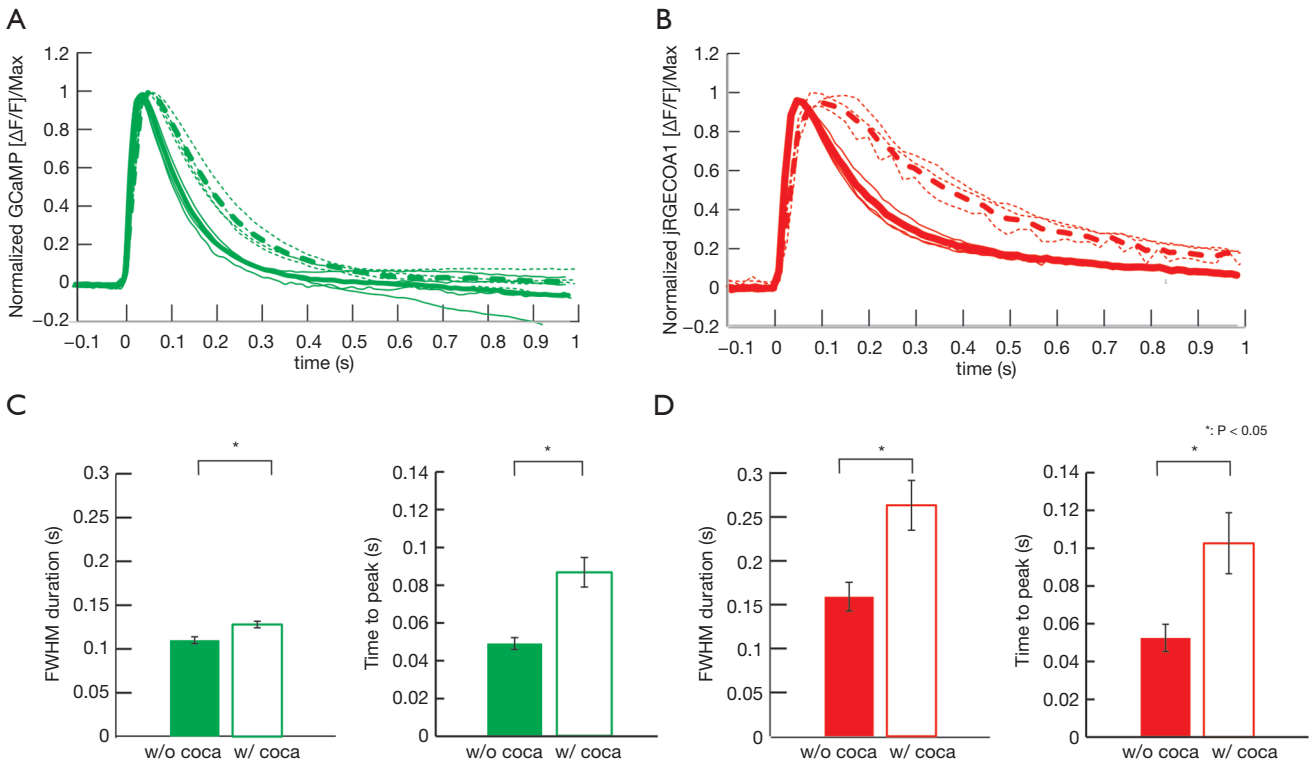

Figure 6 Cocaine's effect on stimulation-evoked Ca^{2+} transient in GCaMP6f and jRGECO1a rats. (A,B) Stimulation-evoked Ca^{2+} transients in GCaMP6f (green) and jREGCO1a (red) expressing neurons before (solid traces) and after cocaine administration (dashed traces); (C,D) FWHM duration and time to peak of neuronal Ca^{2+} transients before (green/red) and after (white) cocaine. Cocaine significantly increased FWHM duration from 0.11±0.003 to 0.13±0.003 s (P=0.01) and time to peak from 0.049±0.003 to 0.09±0.008 s (P=0.04) in GCaMP6f rats, and in jREGCO1a rats from 0.159±0.01 to 0.26±0.03 s for HWHM duration (P=0.03) and from 0.05±0.007 to 0.10±0.016 s for time to peak (P=0.04).

and from 0.05±0.007 to 0.10±0.016 s (P=0.04, n=3) for the jREGCO1a rats.

Discussion and conclusions

In this study, we used optical imaging to assess neuronal Ca^{2+} transients from the somatosensory cortex of rats in response to forepaw electrical stimulations. From the experiments, we were able to systematically analyze the differences of stimulation evoked neuronal Ca^{2+} fluorescence signaling expressed with two different GECIs, i.e., GCaMP6f and jRGECO1a. In addition, we compared stimulation-evoked neuronal Ca^{2+} transients before and after an acute cocaine challenge. In order to examine the neuron counts expressing GCaMP6f or jRGECO1a, ex-vivo confocal fluorescence microscopy was conducted on brain slides from the same animals after the *in vivo* imaging studies. Our results showed no significant difference in the expressing rates uptaken by the neurons between these two groups of animals (*Figure 2E*). To test whether the invasive procedure of a viral injection would influence on the brain responses to sensory stimulation, we recorded the hemodynamic changes (i.e., changes in total hemoglobin concentration, ΔHbT) in the somatosensory cortex to response to sensory stimulations (3 mA/0.03 Hz/0.3 ms). *Figures 3E* and *4E* showed that ΔHbT responded to each stimulus, suggesting that the effects of viral injection on the brain to respond to sensory stimulation were negligible. The results to readily detect ΔHbT response to each single stimulation also illustrate the high sensitivity of our optical system to capture the hemodynamic changes evoked by weak stimulations. The comparison of stimulation-induced ΔHbT changes between jRGECO1a-expressed rats (n=3) and GCaMP6f-expressed rats (n=4) was summarized in

Figure 5, showing no significant differences between the two groups. This indicates the equivalency of the animal model and the physiological responses between the two animal groups. However, for detection of Ca^{2+} signaling, the jRGECO1a-expressed neuronal Ca^{2+} fluorescence exhibited a longer transient time as measured by the FWHM duration than that of the GCaMP6f-expressed neuronal Ca^{2+} (*Figure 5F*) although no significant differences were found in the time to peak (*Figure 5G*) and the peak transient amplitude (*Figure 5H*) between them. Indeed, it has been reported that jRGECO1a has a longer half decay time than GCaMP6f (8), which is in agreement with our findings here.

Thanks to the development of high sensitivity and fast GECIs for brain function studies, our optical imaging enables capturing Ca^{2+} transient from neurons in response to single stimulus in both GCaMP6f and jRGECO1a groups (*Figures 3A,4A*). To ensure the Ca^{2+} fluorescence signals approximately from the same cortical depth within the brain, we used the same viral injection protocol to control the viral delivering into the neurons in a similar location. Specifically in this study, the viral vehicle was inserted to 1.2mm beyond the skull of the cortex (25), which made approximately reached to Layer 4-Layer 5 (LIV-LV) within the cortex (*Figure 2C,D*).

The comparisons before and after an acute cocaine administration (*Figure 6*) show that cocaine delayed and prolonged neuronal Ca^{2+} transient responses evoked by sensory stimulations in both GCaMP6f and jRGECO1a rats. Specifically, the FWHM duration and the time-to-peak in both groups were increased by cocaine (*Figure 6C,D*). Prior microelectrode recording reported that cocaine suppressed the short-latency excitation of cortical neurons in the first 10–25 ms after the electrical stimulation of the whisker pad followed by a postexcitatory inhibition within 25–120 ms after the stimulation (26). However, the long-latency excitation of the cortical neurons was enhanced in 120–300 ms after stimulation in the somatosensory cortex by cocaine. The cocaine-induced redistribution of the latency of neuronal activation might underlie the shifting of $\Delta F/F$ signaling (40–50 ms delay of time to peak after cocaine) and the increase (20–100 ms) of FWHM duration observed in GCaMP6f and jRGECO1a animals. In addition, it has been also reported that acute cocaine depressed cortical activity, including a prolonged membrane depolarization (27). Indeed, we have observed the decrease of cortical spontaneous firing rates resulting from cocaine in anesthetized animals (28-30). However, to the best of our knowledge, this is the first report of the measurement of cocaine's effects on Ca^{2+} transients to single stimulation from a synchronized neuronal ensemble.

Red-shifted GECIs such as jRGECO1a red fluorescence probe could be used with green probes such as GCaMP6f to image the activity and interactions of different cell types such as neurons and astrocytes simultaneously. To do so, these two GECIs need to be virally delivered to a target region of the brain (e.g., the prefrontal cortex or sensory cortex, etc.). For example, if the astrocyte is to be labeled by GCaMP6f, and then the neuron should be labeled with jRGECO1a. The viruses of AAV.Syn.NES-jRGECO1a.WPRE.SV40 and AAV.CAG.FLEX.GCaMP6f.WPRE.SV40 can be delivered into the brain of a GFAP-cre dependent mouse at the same time. After few weeks for expression, the animal can be imaged. A custom-designed emission filters will be needed to synchronize with the excitation of GCaMP and jRGECO1a, respectively, and the images of the green Ca^{2+} fluorescence from astrocytes and red Ca^{2+} signal from neurons in the same field of view of the cortex can be detected.

It has been noted that the hemodynamic changes within the brain might influence on Ca^{2+} fluorescence measurements (18,31) due to the absorbance changes in the biological tissue. To eliminate this artifact, various strategies have been developed, including to conduct the correction in frequency domain (32,33) and in time domain (16,19). However, as we reported recently (19), the single-pulse stimuli sparsely delivered every 30s in between the resting periods, the light absorption change induced by hemodynamic fluctuation was so small that its effect on the Ca^{2+} signal was negligible (e.g., <1% before and after the correction).

In summary, our study demonstrates the capability of optical imaging detection of Ca^{2+} transients by using either jRGECOa1 or GCaMP6f GECI in response to brain stimulation. Our results indicate that both these two GECIs have sufficient sensitivity for tracking single Ca^{2+} transients to measure the cellular activities from the brain *in vivo*. Since these GECIs are emitted at the different wavelengths, green for GCaMP6f and red for jRGECO1a, they can be used simultaneously to characterize the activities of different cell types (e.g., neurons and astrocytes or subtype neurons) to study the brain activation and brain functional changes induced by drugs or diseases.

Acknowledgments

We thank Kevin Clare and Gloria Kim for helping on

ex vivo imaging, and Kathryn Sharer for helping with viral injection. The authors would also like to thank the NIDA drug supply program for providing the cocaine used in this study.

Funding: This research was supported in part by National Institutes of Health grants 2R01 DA029718 (CD & YP), RF1DA048808 (YP & CD), R21DA042597 (CD & YP), and by the NIH NINDS Intramural Program (APK).

Footnote

Provenance and Peer Review: With the arrangement by the Guest Editors and the editorial office, this article has been reviewed by external peers.

Conflicts of Interest: All authors have completed the ICMJE uniform disclosure form (available at http://dx.doi.org/10.21037/qims-20-921). The special issue "Advanced Optical Imaging in Biomedicine" was commissioned by the editorial office without any funding or sponsorship. The authors have no other conflicts of interest to declare.

Ethical Statement: All experiment procedures were approved by the Institutional Animal Care and Use Committees (IACUC) of NIH and Stony Brook University and were performed in accordance with the National Institutes of Health Guide for the Care and Use of Laboratory Animals.

References

1. Chen TW, Wardill TJ, Sun Y, Pulver SR, Renninger SL, Baohan A, Schreiter ER, Kerr RA, Orger MB, Jayaraman V, Looger LL, Svoboda K, Kim DS. Ultrasensitive fluorescent proteins for imaging neuronal activity. Nature 2013;499:295-300.
2. Ahrens MB, Orger MB, Robson DN, Li JM, Keller PJ. Whole-brain functional imaging at cellular resolution using light-sheet microscopy. Nat Methods 2013;10:413-20.
3. Peron SP, Freeman J, Iyer V, Guo C, Svoboda K. A cellular resolution map of barrel cortex activity during tactile behavior. Neuron 2015;86:783-99.
4. Paredes RM, Etzler JC, Watts LT, Zheng W, Lechleiter JD. Chemical calcium indicators. Methods 2008;46:143-51.
5. Tian L, Hires SA, Mao T, Huber D, Chiappe ME, Chalasani SH, Petreanu L, Akerboom J, McKinney SA, Schreiter ER, Bargmann CI, Jayaraman V, Svoboda K, Looger LL. Imaging neural activity in worms, flies and mice with improved GCaMP calcium indicators. Nat Methods 2009;6:875-81.
6. Akerboom J, Chen TW, Wardill TJ, Tian L, Marvin JS, Mutlu S, Calderón NC, Esposti F, Borghuis BG, Sun XR, Gordus A, Orger MB, Portugues R, Engert F, Macklin JJ, Filosa A, Aggarwal A, Kerr RA, Takagi R, Kracun S, Shigetomi E, Khakh BS, Baier H, Lagnado L, Wang SS, Bargmann CI, Kimmel BE, Jayaraman V, Svoboda K, Kim DS, Schreiter ER, Looger LL. Optimization of a GCaMP calcium indicator for neural activity imaging. J Neurosci 2012;32:13819-40.
7. Ohkura M, Sasaki T, Sadakari J, Gengyo-Ando K, Kagawa-Nagamura Y, Kobayashi C, Ikegaya Y, Nakai J. Genetically encoded green fluorescent Ca2+ indicators with improved detectability for neuronal Ca2+ signals. PLoS One 2012;7:e51286.
8. Dana H, Mohar B, Sun Y, Narayan S, Gordus A, Hasseman JP, Tsegaye G, Holt GT, Hu A, Walpita D, Patel R, Macklin JJ, Bargmann CI, Ahrens MB, Schreiter ER, Jayaraman V, Looger LL, Svoboda K, Kim DS. Sensitive red protein calcium indicators for imaging neural activity. eLife 2016;5:e12727.
9. Svoboda K, Block SM. Biological applications of optical forces. Annu Rev Biophys Biomol Struct 1994;23:247-85.
10. Goldstein RZ, Leskovjan AC, Hoff AL, Hitzemann R, Bashan F, Khalsa SS, Wang GJ, Fowler JS, Volkow ND. Severity of neuropsychological impairment in cocaine and alcohol addiction: association with metabolism in the prefrontal cortex. Neuropsychologia 2004;42:1447-58.
11. Lee JH, Telang FW, Springer CS. Abnormal brain activation to visual stimulation in cocaine abusers. Life Sci 2003;73:1953-61.
12. Tomasi D, Goldstein RZ, Telang F, Maloney T, Alia-Klein N, Caparelli EC, Volkow ND. Widespread disruption in brain activation patterns to a working memory task during cocaine abstinence. Brain Res 2007;1171:83-92.
13. George O, Mandyam CD, Wee S, Koob GF. Extended

access to cocaine self-administration produces long-lasting prefrontal cortex-dependent working memory impairments. Neuropsychopharmacology 2008;33:2474-82.
14. Du C, Koretsky AP, Izrailtyan I, Benveniste H. Simultaneous detection of blood volume, oxygenation, and intracellular calcium changes during cerebral ischemia and reperfusion in vivo using diffuse reflectance and fluorescence. J Cereb Blood Flow Metab 2005;25:1078-92.
15. Chen W, Park K, Volkow N, Pan Y, Du C. Cocaine-Induced Abnormal Cerebral Hemodynamic Responses to Forepaw Stimulation Assessed by Integrated Multi-wavelength Spectroimaging and Laser Speckle Contrast Imaging. IEEE J Sel Top Quantum Electron 2016;22:6802608.
16. Yuan Z, Luo Z, Volkow ND, Pan Y, Du C. Imaging separation of neuronal from vascular effects of cocaine on rat cortical brain in vivo. Neuroimage 2011;54:1130-9
17. Dunn AK, Devor A, Dale AM, Boas DA. Spatial extent of oxygen metabolism and hemodynamic changes during functional activation of the rat somatosensory cortex. Neuroimage 2005;27:279-90.
18. Ma Y, Shaik MA, Kim SH, Kozberg MG, Thibodeaux DN, Zhao HT, Yu H, Hillman EM. Wide-field optical mapping of neural activity and brain haemodynamics: considerations and novel approaches. Philos Trans R Soc Lond B Biol Sci 2016;371:20150360.
19. Chen W, Park K, Pan Y, Koretsky AP, Du C. Interactions between stimuli-evoked cortical activity and spontaneous low frequency oscillations measured with neuronal calcium. Neuroimage 2020;210:116554.
20. Stefanovic B, Hutchinson E, Yakovleva V, Schram V, Russell JT, Belluscio L, Koretsky AP, Silva AC. Functional reactivity of cerebral capillaries. J Cereb Blood Flow Metab 2008;28:961-72.
21. Hutchinson EB, Stefanovic B, Koretsky AP, Silva AC. Spatial flow-volume dissociation of the cerebral microcirculatory response to mild hypercapnia. Neuroimage 2006;32:520-30.
22. Silva AC, Koretsky AP, Duyn JH. Functional MRI impulse response for BOLD and CBV contrast in rat somatosensory cortex. Magn Reson Med 2007;57:1110-8.
23. Gu X, Chen W, You J, Koretsky AP, Volkow ND, Pan Y, Du C. Long-term optical imaging of neurovascular coupling in mouse cortex using GCaMP6f and intrinsic hemodynamic signals. Neuroimage 2018;165:251-64.
24. Gu X, Chen W, Volkow ND, Koretsky AP, Du C, Pan Y. Synchronized Astrocytic Ca2+ Responses in Neurovascular Coupling during Somatosensory Stimulation and for the Resting State. Cell Rep 2018;23:3878-90.
25. Paxinos G, Franklin KJ. The Mouse Brain in Stereotaxic Coordinates. San Diego: Academic Press, 2001.
26. Drouin C, Waterhouse BD. Cocaine-induced vs. Behaviour-Related Alterations of Spontaneous and Evoked Discharge of Somatosensory Cortical Neurons. Eur J Neurosci 2004;19:1016-26.
27. Trantham-Davidson H, Lavin A. Acute cocaine administration depresses cortical activity. Neuropsychopharmacology 2004;29:2046-51.
28. Chen W, Liu P, Volkow ND, Pan Y, Du C. Cocaine attenuates blood flow but not neuronal responses to stimulation while preserving neurovascular coupling for resting brain activity. Mol Psychiatry 2016;21:1408-16.
29. Chen W, Volkow ND, Li J, Pan Y, Du C. Cocaine Decreases Spontaneous Neuronal Activity and Increases Low-Frequency Neuronal and Hemodynamic Cortical Oscillations. Cereb Cortex 2019;29:1594-606.
30. Park K, Chen W, Volkow ND, Allen CP, Pan Y, Du C. Hemodynamic and neuronal responses to cocaine differ in awake versus anesthetized animals: Optical brain imaging study. Neuroimage 2019;188:188-97.
31. Wright PW, Brier LM, Bauer AQ, Baxter GA, Kraft AW, Reisman MD, Bice AR, Snyder AZ, Lee JM, Culver JP. Functional connectivity structure of cortical calcium dynamics in anesthetized and awake mice. PLoS One 2017;12:e0185759.
32. Du C, Pan Y, MacGowan GA, Koretsky AP. Decreasing motion artifacts in calcium-dependent fluorescence transients from the perfused mouse heart using frequency filtering. Cell Calcium 2004;35:141-53.
33. Du C, Volkow ND, Koretsky AP, Pan Y. Low-frequency calcium oscillations accompany deoxyhemoglobin oscillations in rat somatosensory cortex. Proc Natl Acad Sci U S A 2014;111:E4677-86.

Cite this article as: Park K, Liyanage AC, Koretsky AP, Pan Y, Du C. Optical imaging of stimulation-evoked cortical activity using GCaMP6f and jRGECO1a. Quant Imaging Med Surg 2021;11(3):998-1009. doi: 10.21037/qims-20-921

